Superalloys 2008
Roger C. Reed, Kenneth A. Green, Pierre Caron, Timothy P. Gabb, Michael G. Fahrmann, Eric S. Huron and Shiela A. Woodard
TMS (The Minerals, Metals & Materials Society), 2008

LONG TERM COARSENING IN RENÉ 80 Ni-BASE SUPERALLOY

Despina Hadjiapostolidou, Barbara A. Shollock

Department of Materials, Imperial College London, Exhibition Road, London SW7 2AZ, UK

Keywords: long-term aging, René 80, coarsening, diffusion-controlled growth, interface-controlled growth, particle size distribution.

Abstract

The influence of temperature and time on the microstructure of René 80 after long term aging was examined. The alloy was subjected to aging heat treatments at five different temperatures ranging from 850°C to 1,050°C for five different times 1000h, 2000h, 5000h, 10000h and 20000h. The microstructural evolution was characterized with scanning electron microscopy. The average particle radius of γ' precipitates was calculated and the growth of the precipitates was compared to both the cube and square rate laws in an attempt to identify the dominant mechanism. Assuming diffusion controlled growth, the coarsening activation energy was calculated to be 127 kJ/mol. The particle size distributions (PSD) for the populations of γ' precipitates were compared with theoretical models. There was generally a poor fit between the experimentally measured values and the theoretical distribution but the LSEM model, which accounts for encounters between particles, resulted in the best fit.

Introduction

Ni-based superalloys owe their remarkable properties to the γ' phase precipitation. The volume fraction, size, shape and distribution of these precipitates strongly affect the properties of these alloys. The microstructure changes with time and temperature and coarsening occurs during service, altering the properties of components and determining their service life. The microstructural changes in these alloys have been extensively studied; most studies focused on the growth kinetics for short times compared to the life of turbine components. It is important to investigate the microstructural evolution over long aging times and to understand the mechanisms and growth kinetics in order to have a realistic estimation of the service life. This is especially important in the case of land-based turbines that operate for very long times.

There are two mechanisms for particle growth [1]: i) the mechanism of diffusion controlled growth in which coarsening is described by the cube rate law

$$r_{av}^3 \propto K_1 t \quad (1)$$

where r_{av} is the average particle radius at time t and K_1 is the diffusion controlled coarsening constant and ii) the mechanism of interface reaction controlled growth in which coarsening follows the square rate law

$$r_{av}^2 \propto K_2 t \quad (2)$$

where r_{av} is again the average particle radius at time t and K_2 is the interface controlled coarsening constant.

In the case of the first mechanism the coarsening constant K_1 is temperature dependant and can be described by

$$K_1 T \propto \exp(-Q/RT) \quad (3)$$

$$\ln(K_1 T) \propto \text{constant} - (Q/R)(1/T) \quad (4)$$

where T is the temperature in K, R is the gas constant and Q is the activation energy for coarsening. From the graph of $\ln(K_1 T) - 1/T$ the activation energy for coarsening can be calculated.

It is generally accepted that for short-term coarsening the cube rate law operates. For long term aging of superalloys, however, little research has been reported, and the cube rate law is usually assumed [2-5]. McLean [1] extrapolated short time data collected from previous studies for a number of Ni-Al (5.68-9.9 wt.% Al), Ni-Cr-Al (14.2-17.5 wt.% Cr, 2.7-4.9 wt.% Al) alloys and IN738 to long times.

In the present work the influence of temperature and time on the microstructure after long term aging in René 80 was investigated. The microstructural evolution was characterized with scanning electron microscopy and particle size evolution was compared with both the diffusion and interface controlled growth laws for coarsening. The particle size distributions were compared with theoretical models.

Experimental Procedure

The alloy used was René 80, a polycrystalline Ni-based cast superalloy used for gas turbine blades because it shows high mechanical properties (rupture stress at 870°C 350MPa for 100h and 240MPa for 1000h, at 980°C 160MPa for 100h and 105MPa for 1000h) [6] as well as microstructural stability during high temperature operation. The composition of the alloy is shown in Table I.

Table I: Chemical composition of René 80 in wt% [6].

Co	Cr	Mo	W	Ti	Al	C	B	Zr	Ni
9.5	14	4	4	5	3	.17	.015	.03	Bal

The samples underwent the standard heat treatment in vacuum or in Ar or He atmosphere prior to the final aging. The standard heat treatment was: 1190-1218°C for 2 hours, cooling down to 1080-1107°C with cooling rate of 11°C/min by furnace cooling and hold for 4 hours. Then the temperature was dropped down to

650°C with cooling rate of 7.5°C/min by furnace cooling and then dropped down to room temperature. The final step was heating at 845°C for 16 hours.

The resulting microstructure after the standard heat treatment is bimodal and consists of cuboidal primary γ' and spheroidal secondary γ', as illustrated in Figure 1. Following this heat treatment schedule, 24 different aging treatments were performed in air atmosphere at 850°C, 900°C, 950°C, 1000°C for 5 aging times up to 20000 h and at 1050°C for 4 aging times up to 10000 h (Table II), followed by air cooling.

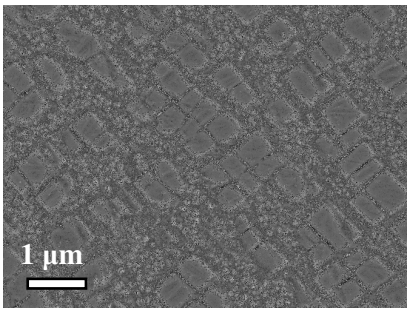

Figure 1: Initial microstructure of René 80 after the standard heat treatment.

Table II: Aging heat treatments.

T(°C)	t (h)
850	1000, 2000, 5000, 10000, 20000
900	1000, 2000, 5000, 10000, 20000
950	1000, 2000, 5000, 10000, 20000
1000	1000, 2000, 5000, 10000, 20000
1050	1000, 2000, 5000, 10000

Sections of each sample were polished and electro-etched with a solution of phosphoric acid (2 vol.% - 10 vol.%) at room temperature and at 2V, which resulted in a preferentially etching of the γ phase. Subsequently, the samples were examined using a LEO Gemini 1525 field emission gun scanning electron microscope (FEGSEM). The resulting micrographs were analyzed using the ImageJ software. In an attempt to minimize errors in particle size measurements, grains with a nominal [001] orientation where selected for analysis. While for low temperatures and short aging times, grains with orientation close to [001] can be easily identified by the shape of the γ' precipitates, as coarsening proceeds the precipitate shape becomes increasingly irregular. Finally, five micrographs from five different grains were analyzed for each sample to minimize the errors arising form different grain orientation. The area of each precipitate was measured and their size was calculated as the radius of a circle with the same area. The secondary γ' precipitates were not measured. After the radii of all the primary precipitates were calculated, the average precipitate radius r_{av} was found for each sample.

Results

Evolution of microstructure

The micrographs showing the evolution of the microstructure for aging times 1000 h, 5000 h and 20000 h and temperatures 850°C - 1050°C are presented in Figure 4. For samples aged at 850°C and 900°C for 1000 h, there is still some evidence of the initial bimodal distribution. Coalescence becomes evident after 5000 h at 850°C and after 1000 h for 900°C - 1000°C. The shape of the particles changes from cubic to rounded cubic to irregular. The irregular morphology indicates that apart from coarsening, coalescence also takes place. L- and U- shaped precipitates as well as precipitates with aspect ratios greater than 1 are probably the result of coalescence of a number of originally smaller precipitates. The precipitate size increases both with time and temperature up to 1000°C. At 1050°C, the size of the primary γ' decreases. Further examination revealed fine γ' precipitation in the interparticle spacing, as shown in the micrograph in Figure 2.

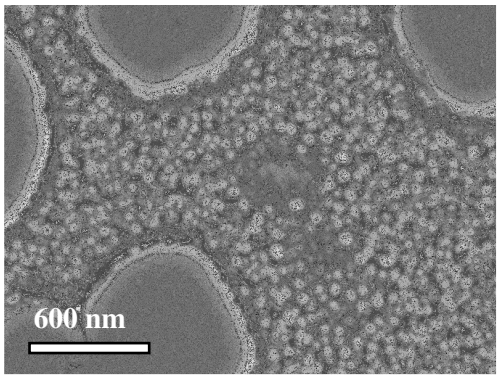

Figure 2: Primary γ' and secondary γ' in the sample that was aged at 1050°C for 5000 h.

Precipitate size evolution

The results for the evolution of the average precipitate size are shown in Figure 5. The 1000°C data are divided in two regions; one where the particle size increases (● 1000°C) and one where there is a decrease in particle size (○ 1000°C-b). Errors arise from sectioning effects imposed by measurements from 2-dimensional images. This is particularly true in the case of L- and U-shaped precipitates. In these cases, depending of the plane of view, we measure one or two small particles instead of one larger (Figure 3). Another source of errors is the grain orientation. As mentioned earlier, five micrographs from different grains were analyzed to minimize these errors. Furthermore there are cases of particles being very close together, making it difficult to decide whether they are separate particles or have coalesced. These errors could not be quantified.

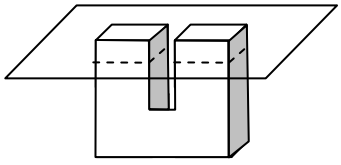

Figure 3: Schematic example of errors in measurements arising from U-shaped particles depending on the plane of view.

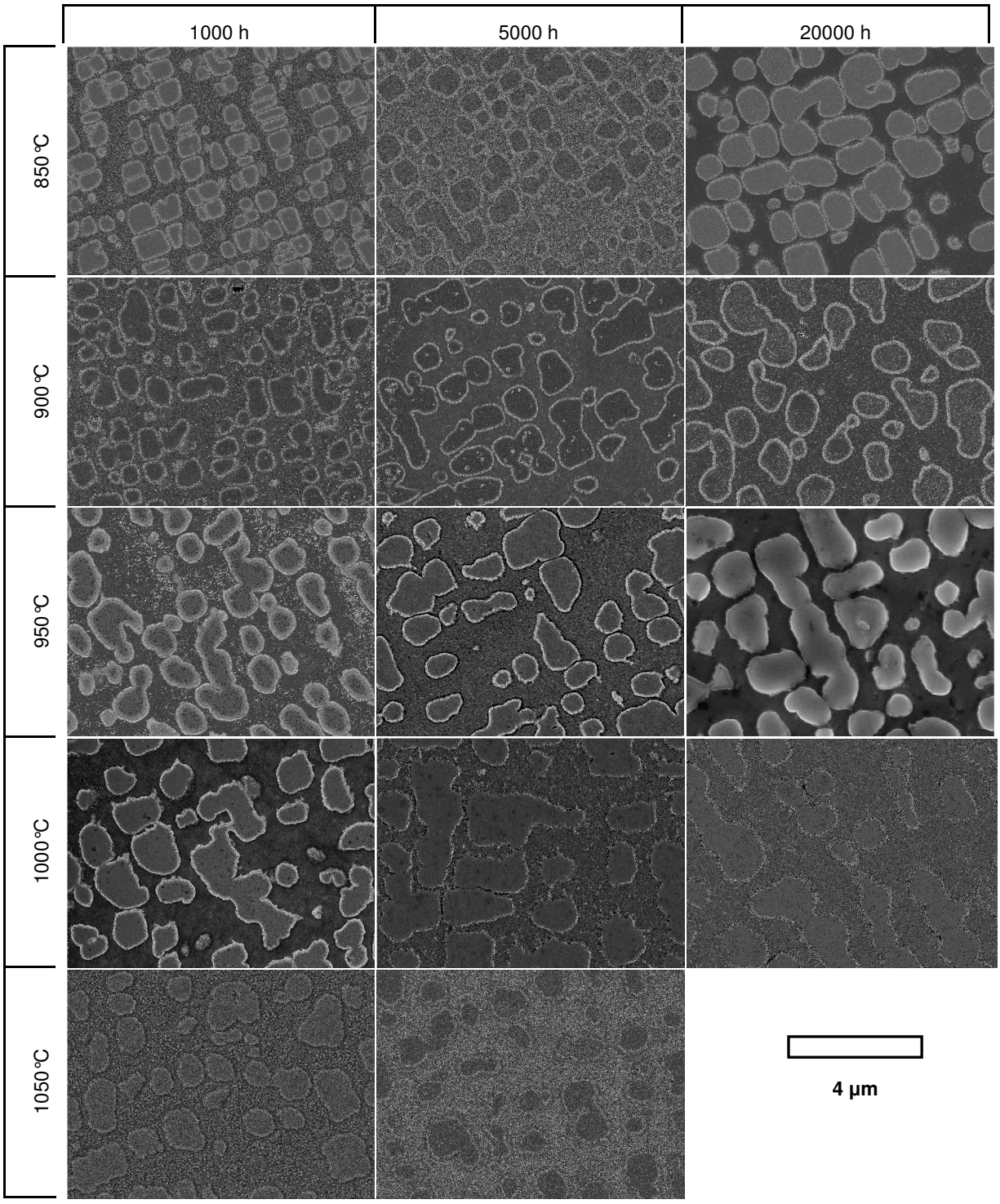

Figure 4: Evolution of microstructure in René 80.

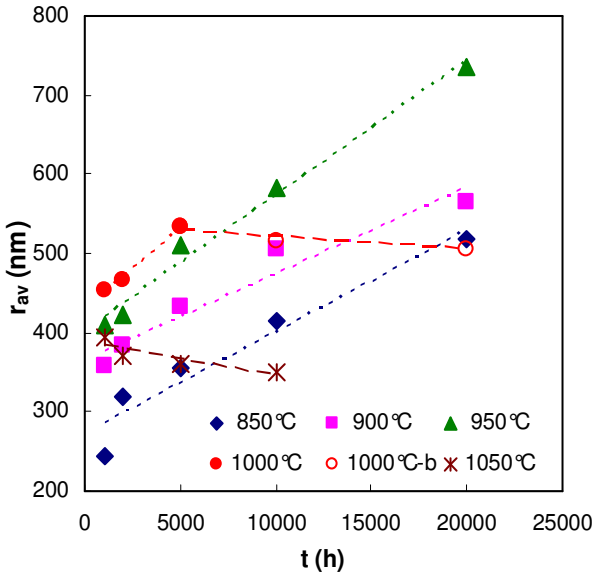

Figure 5: Evolution of average precipitate size.

Analysis and Discussion

Precipitate size evolution

The results in Figure 5 are in agreement with the SEM observations (Figure 4). Coarsening is evident at all aging times for 850°C - 950°C. At 1000°C for times up to 5000 h the precipitate size increases, but after 5000 h (line 1000°C-b) the average size of the precipitates decreases. The same decrease in average precipitate size is also observed for 1050°C and aging times from 1000 h to 10000 h. Since the size of the small secondary γ' were not measured, this decrease must result from the partial re-solution of primary γ' and the precipitation of secondary γ' in the interparticle spacing.

Size saturation was observed for experimental Ni-Al-Ta-Mo alloys by MacKay & Nathal [5] and for Nimonic 80A at 810°C after 6000h, at 870°C after 5000h and at 930°C after 1700h as well for IN939 at 930°C after 2700°C [2]. In the first study [5] the size saturation was viewed as an inherent stabilization of the microstructure in alloys with highly negative misfit (δ=–0.72%) and was attributed to dislocation networks forming at the γ-γ' interfaces. The reported value of misfit for René 80 however is positive and smaller (δ=0.3% at 982°C, [7]), but this value is without reference and not very reliable. In the same study [5] the size saturation coincided with the coalescence of γ' precipitates and the formation of plates. This is not the case in this study, since coalescence occurs much earlier than the observed size decrease. In the second study [2], the size saturation was attributed to either or both of two factors: the time-temperature re-solution effect and the observed small number of particles per grain for the longest time samples. The time-temperature re-solution effect agrees with the partial dissolution observed in this study for the samples aged at 1000°C for 10000 h - 20000 h and at 1050°C for 1000 h – 10000 h, but in this case there is no size saturation but in fact size decrease. Re-solution is also supported by the area fraction measurements of the primary γ' given in Figure 6. For 1050°C there is a clear tendency for decrease in area fraction and for 1000°C the same tendency occurs after 5000h. The area fraction measurements for 900°C are also given for comparison, which show that the area fraction is stable at this temperature. Footner & Richards [8] reported that there is considerable weight of practical experience from industrial users that re-solution occurs over long times at high working temperatures, close to the solution temperature. In the case of René 80 the solution temperature is about 1200°C. According to the results of this study, re-solution occurs earlier at higher temperatures (after 5000h at 1000°C and after 1000h at 1050°C).

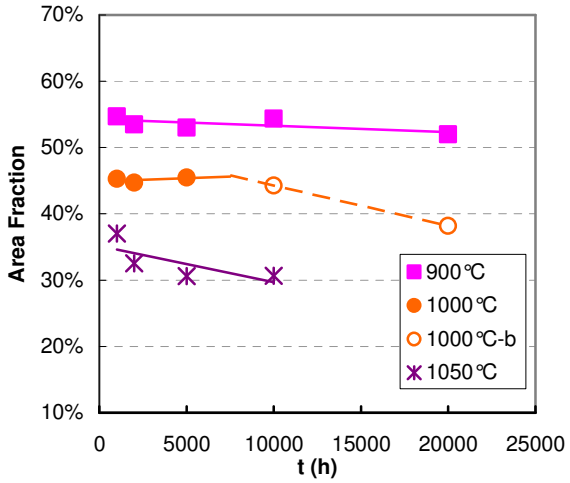

Figure 6: Area fraction measurements of primary γ' for aging temperatures 900°C, 1000°C and 1050°C.

Rate controlling mechanism

The results for the average particle size were used to assess the rate limiting mechanism. If growth is interface controlled, then the square rate law (equation 2) applies, whereas if growth is diffusion controlled it follows the cube rate law (equation 1). For the samples aged at 850°C - 950°C for 1000 h – 20000 h and at 1000°C for 1000 h - 5000 h, both equations were plotted and the fitting parameter R^2 are listed in Table III. An example of the graphs is shown in Figure 7 for growth at 850°C. When comparing the fitting parameters of the two rate controlling mechanisms we see that for the lowest temperatures, 850°C and 900°C, the fit is slightly better for the cube rate law (2nd decimal), while for the higher temperatures, 950°C and 1000°C, the square rate law gives a slightly better fit (3rd decimal). It is important to note that for 1000°C the data from the samples that were aged for 10000 h or more, where dissolution occurs, were excluded. No definitive conclusions can be drawn from this comparison; none of the two mechanisms is clearly dominant.

Table III: Values of the fitting parameter R^2 for the diffusion and interface controlled rate laws.

T	*850°C*	*900°C*	*950°C*	*1000°C*
Interface controlled	0.9754	0.9615	0.9905	0.9891
Diffusion controlled	0.9898	0.9785	0.9847	0.9869

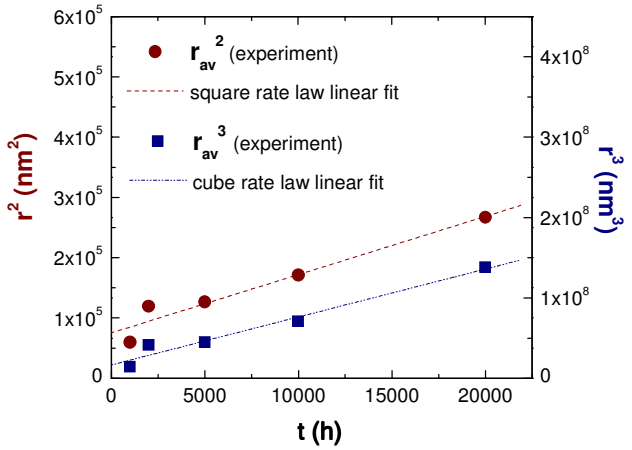

Figure 7: Comparison between the two mechanisms of growth at 850°C.

It has been reported for René 80 [9] that at 870°C no more coarsening occurs between 1000 and 1750 h. Figure 5 shows that the average particle size at 850°C continues to increase after 1000 h. The data reported for short-term aging were adjusted and plotted together with the results of the current study. The reported data for 870°C were combined with the 850°C results and the 980°C data were combined with the 950°C current results. Although the temperatures are not exactly the same, they are close enough to compare the coarsening rate. The combined plots are shown in Figure 8. It is obvious that coarsening continues after 2000 h, although at a slower rate.

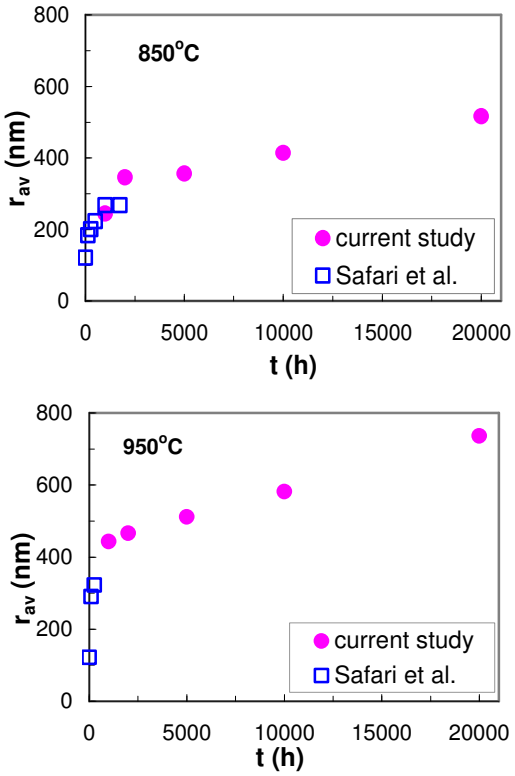

Figure 8: Combined data of average particle size for short-term [9] and long-term aging at 850°C and 950°C for René 80.

For 950°C the equations of both interface and diffusion controlled coarsening were plotted again, this time using the combined data (Figure 9). The fitting was performed in two regions. One for short times (0-2000h) and one for long times (2000h-20000h) and the resulting fitting parameters R^2 for each region and temperature is given in Table IV. At 950°C, the cube rate law fits better the short time data and the square rate law fits the long time data better (2nd decimal).

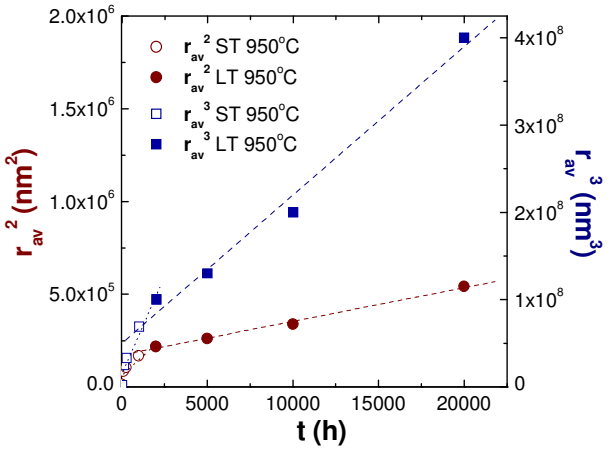

Figure 9: Comparison between the two mechanisms of growth at 950°C.

Table IV: Values of the fitting parameter R^2 for the diffusion and interface controlled rate laws for short (ST: 0-2000h) and long (LT: 2000h-20000h) aging times at 950°C.

T	*950°C*	
	ST	LT
Interface controlled	0.9269	0.9971
Diffusion controlled	0.9707	0.9928

Activation energy for coarsening

Assuming that the cube rate law, in common with previous reported research [2-5], is dominant, we can calculate the activation energy for coarsening, Q, from equation 4 with the help of the graph shown in Figure 10. The value of the activation energy for coarsening was calculated to be Q = 127 kJ/mol. This analysis considers only data from 850°C – 950°C to exclude re-solutioning effects.

The calculated value of the activation energy for coarsening is much lower than the activation energies for diffusion of Al in Ni (270 kJ/mol) and Ti in Ni (257 kJ/mol) [10] and the reported value for René 80 for short term aging (218 kJ/mol) [9]. As it is illustrated in Table V, the reported values of the coarsening activation energy for several Ni-base alloys vary, even for the same alloy as in the case of IN738LC with reported values ranging from 150 to 300 kJ/mol. For this alloy Balikci et al. [11] calculated different activation energies for 2 temperature ranges, but they also found different values between furnace cooled and water quenched samples.

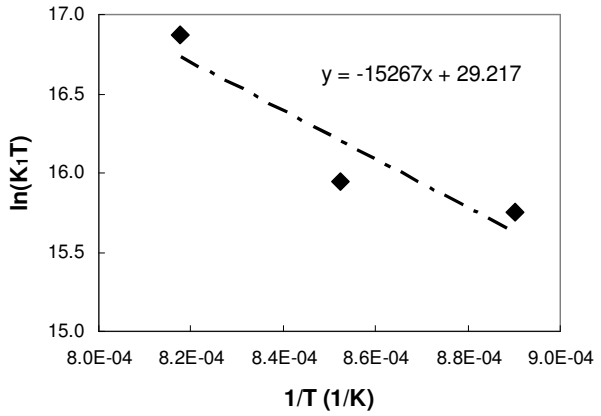

Figure 10: Plot of $\ln(K_1T)$ versus 1/T for the calculation of the activation energy, Q.

Table V: Reported activation energies for coarsening of various Ni-base alloys.

Alloy	*Q (kJ/mol)*	*T (°C)*	*max t (h)*	*Reference*
Ni-Al	270			[12]
Ni-Ti	282	525-692		[13]
Udimet 520	104	700-800	100	[14]
Nimonic 80A	274	750-930	15000	[2]
Nimonic 90	257	750-930	15000	[2]
Nimonic 105	263	750-930	15000	[2]
IN939	265	750-930	15000	[2]
IN738LC	150 150 191 292 350	850-1050 750-1050 (FC) 850-1050 (WQ) 1050-1120 (FC) 1050-1120 (WQ)	600 24 24 24 24	[15] [11] [11] [11] [11]
René 80	218 127	871-982 850-950	1750 20000	[9] present work

Particle Size Distribution (PSD)

The experimental particle size distributions were compared with the theoretical curves of the Lifshitz-Slyozov-Wagner (LSW, 0% volume fraction), the Modified Lifshitz-Slyozov-Wagner (MLSW, 100% volume fraction) and the Lifshitz-Slyozov Encounter Modified (LSEM, 40% volume fraction) models. The LSW model assumes zero volume fraction of precipitate phase, a problem which the MLSW tries to address by introducing a dependence of the coarsening rate constant and the PSD on the precipitate volume fraction. The LSEM also considers the effect of volume fraction and includes the effect of encounters or coalescence events between particles.

Figure 11 shows the PSDs for the samples aged at 850°C for 1000 h, 5000 h and 20000 h. As can be seen, for the 1000 h sample the PSD is flatter and shifted to the left due to the influence of the original bimodal distribution. All distributions were broader than the theoretical ones. Generally, there was poor fit of the experimental distributions with the theoretical curves. The LSEM model, which accounts for encounters between particles, gave overall the best fit as the predicted distribution is broader and more symmetric than the LSW and MLSW curves.

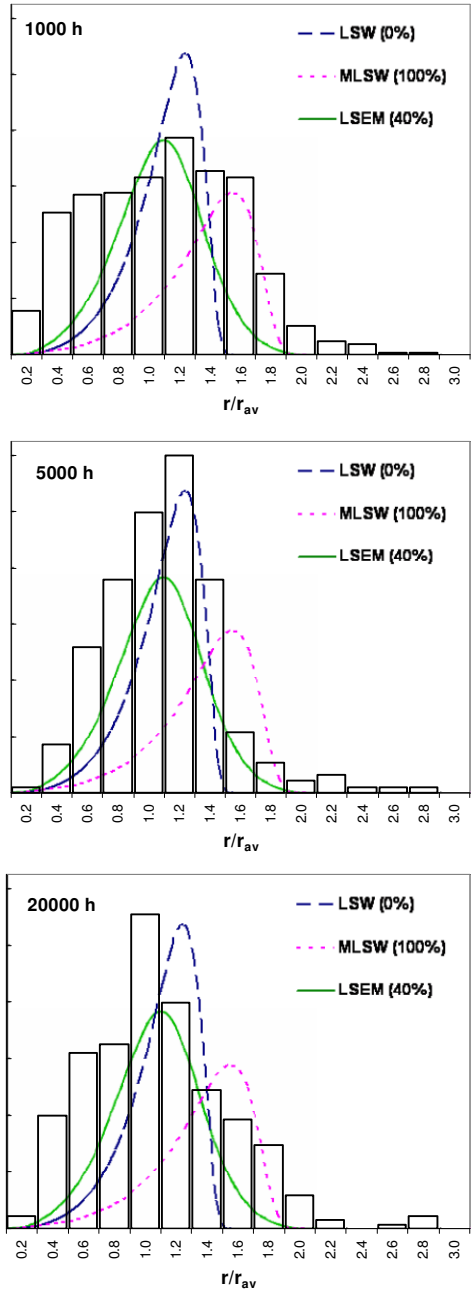

Figure 11: Particle size distributions for 850°C after 1000 h, 5000 h and 20000 h.

Conclusions

The evolution of microstructure after long-term aging observed in René 80 consists of an initial coarsening where the primary γ' grows at the expense of the small secondary γ'. This is followed by coalescence of the γ' precipitates. The average particle size increased for all aging times (1000 h – 20000 h) for temperatures up to 950°C, and at 1000°C up to 5000 h. At 1050°C for all aging times (1000 h – 10000 h) and at 1000°C after 10000 h, partial dissolution of the primary γ' was observed and precipitation of γ' in the matrix. The measurements of the average particle size were compared to both interface and diffusion controlled growth and no mechanism seems clearly dominant, although the cube rate law gave slightly better fit for lower temperatures and the square rate law had a slightly better fit for higher temperatures. The activation energy for coarsening was calculated to be 127 kJ/mol. There was poor fit between the experimental particle size distributions and the ones predicted by the LSW, MLSW and LSEM models, but the LSEM curve resulted in the overall better fit.

Acknowledgements

The authors would like to thank EPSRC (EP/C536312/1) for the financial support and RWE npower for providing the material for this study.

References

1. McLean, D., "Predicting growth of γ' in nickel alloys," *Metal Science*, 18 (1984), 249.

2. Footner, P.K. and B.P. Richards, "Long - term growth of superalloy γ' particles," *Journal of Materials Science*, 17 (1982), 2141-2153.

3. Ges, A.A., "Long term coarsening of γ′ precipitates in a Ni-base superalloy," *Journal of Materials Science*, 32 (1997), 3687-3691.

4. Moshtaghin, R.S. and S. Asgari, "Growth kinetics of γ' precipitates in superalloy IN-738LC during long term aging," *Materials and Design*, 24 (2003), 325-330.

5. MacKay, R.A. and M.V. Nathal, "γ' coarsening in high volume fraction nickel-base alloys," *Acta Metallurgica Et Materialia*, 38 (1990), 993-1005.

6. *Metals Handbook Desk edition*. 2nd ed. (1998) [cited: 2007], Available from: http://products.asminternational.org/hbk/index.jsp.

7. Safari, J. and S. Nategh, "On the heat treatment of Rene-80 nickel-base superalloy," *Journal of Materials Processing Technology*, 176 (2006), 240-250.

8. Footner, P.K.P.K., "Reply to 'Comments on "Long term growth of γ′ particles" '," *Journal of Materials Science*, 18 (1983), 1896-1897.

9. Safari, J., S. Nategh and M. McLean, "Evolution of microstructure of nickel base superalloy at high temperatures," *Materials science and technology*, 22 (2006), 888-898.

10. Stevens, R.A. and P.E.J. Flewitt, "The effects of γ' precipitate coarsening during isothermal aging and creep of the Nickel-base superalloy IN-738," *Materials Science and Engineering*, 37 (1979), 237-247.

11. Balikci, E., "Influence of various heat treatments on the microstructure of polycrystalline IN738LC," *Metallurgical and Materials Transactions; A; Physical Metallurgy and Materials Science*, 28 (1997), 1993-2003.

12. Ardell, A.J. and R.B. Nicholson, "The coarsening of γ' in Ni-Al alloys," *Journal of Physics and Chemistry of Solids*, 27 (1966), 1793-1794.

13. Ardell, A.J., "The growth of gamma prime precipitates in aged Ni-Ti alloys," *Metallurgical Transactions*, 1 (1970), 525-534.

14. Jahazi, M. and A.R. Mashreghi, "Dissolution and precipitation kinetics of γ' in nickel base superalloy Udimet 520," *Materials science and technology*, 18 (2002), 458-462.

15. Rosenthal, R. and D.R.F. West, "Continuous γ' precipitation in directionally solidified IN738 LC alloy," *Materials science and technology*, 15 (1999), 1387-1394.